

A model for the temperature dependence of photoluminescence from self-assembled quantum dots*

Bhavtosh Bansal^{†‡}

*Department of Condensed Matter Physics and Materials Science, Tata Institute of Fundamental Research,
1 Homi Bhabha Road, Mumbai-400005, India.*

(Dated: February 6, 2008)

Photo-excited carriers, distributed among the localized states of self-assembled quantum dots, often show very anomalous temperature dependent photoluminescence characteristics. The temperature dependence of the peak emission energy may be non-monotonic and the emission linewidth can get narrower with increasing temperature. This paper describes a quasi-thermodynamic model that naturally explains these observations. Specifically, we introduce a temperature dependent function to parameterize the degree of thermalization of carriers. This function allows us to continuously interpolate between the well-defined low and high temperature limits of the carrier distribution function and describe the observed anomalies in the photoluminescence spectra with just two fitting parameters. We show that the description is equivalent to assuming that the partially thermalized carriers continue to be described by equilibrium statistics, but with a higher effective temperature. Our treatment of the problem is computationally simpler than the usually employed rate equations based analyses [e.g. Sanguinetti, et al. Phys. Rev. B **60**, 8276 (1999)], which typically also have many more under-determined fitting parameters. The model is extended to quantum dots with a bimodal size distribution.

I. INTRODUCTION

Photoluminescence(PL) spectroscopy has perhaps been the most extensively used characterization tool for self-assembled quantum dots (QD)(1; 2). This is due to the relative ease of the measurement, the information it yields about the extent of quantum confinement and inhomogeneous broadening of the density of states and its very direct relevance in assessing the use of these structures in QD lasers.

The temperature dependent PL spectra in self-assembled QD have certain characteristic anomalies(3; 4; 5; 6; 7; 8; 9). At low temperatures, the linewidth of emission generally decreases with increasing sample temperature. The dependence of linewidth may also be non-monotonic with a minimum at an intermediate temperature. Secondly, the energy value corresponding to the peak of the emission spectrum from an ensemble of dots is typically observed to decrease faster with temperature than what is characteristic of either the bulk material or individual dots. It is now well recognized that both these anomalies are due to the non-thermal nature of the distribution of photoexcited carriers(5; 11; 12). Energetically distributed bound states corresponding to QD of different sizes can act as trapping centers for photoexcited carriers. These electron-hole pairs, excited high up in energy by the pump laser can rapidly relax and get captured into the local potential minima in a random way. At low

temperatures, the finite recombination times may not be long enough for these carriers to cross the local potential minima and access the lowest energy (quasi-thermal) state, whereas at higher temperatures the distribution can be expected to have better thermalized.

Although these essential facts about the carrier dynamics responsible for the temperature dependent anomalies, are well understood(12), modeling these processes, even in a completely classical sense in terms of rate equation based models(8), has turned out to be rather cumbersome. The rate equations(13) attempt to extract out the most important trapping and escape processes with a characteristic activation energy associated with each(8; 9; 10). While this approach is both physical and can yield reasonable fits to the data, one typically requires a large number of underdetermined parameters (rate constants, activation energies, etc.) to explain the experimental data. Most of these parameters may not be directly accessible to experimental determination even in a time resolved measurement. In our opinion, the study of carrier dynamics is best tackled by the more microscopic quantum mechanical models(12), while for describing a steady state PL experiment something simpler should suffice.

The purpose of this paper is to attempt a physically motivated semi-empirical alternative that would allow for direct modelling of the experimental data in terms of small number of fitting parameters. We show that this is easily achieved by extending the carrier thermalization model(14) for Stokes' shift in mismatched alloy quantum wells. A qualitative description(5; 11) of the picture already exists in literature. Our model is equivalent to an equilibrium description for localized carriers in terms of an effective temperature.

*Submitted to Journal of Applied Physics: February 2006

[†]Electronic Address: Bhavtosh.Bansal@fys.kuleuven.be

[‡]Present Address: INPAC-Institute for Nanoscale Physics and Chemistry, Pulsed Fields Group, Katholieke Universiteit Leuven, Celestijnenlaan 200D, Leuven B-3001, Belgium.

II. THEORY

A. Formulation of the model

Consider a semiconductor heterostructure sample, containing say, $\sim 10^{10} \text{ cm}^{-2}$ InAs quantum dots within GaAs matrix, that is homogeneous on the macroscopic scale. The surface features appear with a size distribution, which when unimodal, is generally well described by a Gaussian function(15; 16). Thus the mean lateral size a_0 and the variance $\sigma^2/2$ completely determine the morphology of a sample if, for simplicity, all the dots are assumed to be of similar shape with the same aspect ratio. Even within the assumption of a lack of phase coherent coupling between different quantum dots, the dependence of the ground state transition energy $E_t(a)$ on the size and shape of the dot is rendered quite non-trivial for such heterostructure samples. This is due to the finiteness of the energy barriers at materials interface, non-spherical shapes and the complicated strain distribution within the dot. Furthermore since InAs is a ‘narrow gap’ semiconductor and the confinement energies can be even twice as much as the energy gap, one should expect an active participation of many bands in determining the energy levels. The problem of determining the size dependence of the energy levels is therefore best treated numerically(17). Within a semi-empirical approach, one may then attempt a fit to these numerically calculated transition energies to a single band effective mass-like equation, where the confinement causes an increase in the effective energy gap, but now with the exact values of the parameters determined by a fit(18) to the more precise numerical results. For instance, the size (basal length of the pyramid) dependence of the transition energies as calculated by Grundmann et al.(17) can be quite well described by a relation of the kind

$$E_T(a) = E_g + A/a^k. \quad (1)$$

Fixing E_g at 0.42 eV, the low temperature bandgap of InAs, $A = 2.37 \text{ eV nm}^{1/2}$ and $k = 0.5$ provided a good fit to the calculations in reference (17). Equipped with a relationship between the transition energies and the dot sizes, one may immediately write down the expression for the optical density of states and the absorption coefficient of the ensemble as a sum of absorption by individual quantum dots. The absorption coefficient $\alpha(E, a)$, corresponding to a single dot is essentially the product of the optical matrix element with the size dependent transition energy. The density of states is therefore peaked at this resonance energy with a Lorentzian (19) lineshape due to the finite lifetime introduced by phonon and other scattering processes. This homogeneous broadening γ_e of the energies of individual quantum dots is typically less than a millielectronvolt and is completely drowned by the ensemble inhomogeneity effects which give at least an order of magnitude larger contribution to the optical density of states. One may conveniently take the limit $\gamma_e \rightarrow 0$ and replace the Lorentzian by a delta function.

The dipole matrix element $|d_{cv}|$ would also be, in general, dependent on the effective size of the exciton relative to the quantum dot volume. We assume(18) that $|d_{cv}|^2 \sim a^{-m}$. With these approximations, the ground state interband absorption from the complete ensemble quantum dots with a Gaussian size distribution of mean a_0 and variance $\sigma^2/2$ may be written as

$$\alpha = C \int_0^\infty a^{-m} e^{-(a-a_0)^2/\sigma^2} \delta[h\nu - E_T(a)] da. \quad (2)$$

The constant C clubs together the normalization of the probability distribution function and the other size and energy independent parameters.

The above integral is easily evaluated by collapsing the delta function after making a suitable change of variables and plugging in the relationship between the dot size and ground state transition energy given by equation 1. For the time being one may proceed without substituting the numerical values of k , A and E_g to keep the treatment general. Integration of equation 2 yields (up to energy independent constants)

$$\alpha(E) \propto e^{-\frac{1}{\sigma^2} \left[\left(\frac{A}{E-E_g} \right)^{1/k} - \left(\frac{A}{E_0-E_g} \right)^{1/k} \right]^2} \left[\frac{A}{E_0-E_g} \right]^\chi. \quad (3)$$

$\chi = (k+1-m)/k$ and E_0 is the transition energy associated with the dot of size a_0 .

In a typical low temperature non-resonant PL experiment, the carriers are generated well above the transition energies, typically within the region of the matrix and then they quickly relax to the localized states within the quantum dots. In general, one may expect that the trapping efficiency of larger dots may be larger by the factor of a^s . This should be multiplied within the integrand in equation 2 with the consequence that equation 3 also describes the *low temperature* PL spectra but with a new value of $\chi = (k+1-m+s)/k$. This establishes the general form of the low temperature PL spectra in terms of the quantum dot size distribution and the corresponding exciton energies. At higher temperatures, the PL spectra can significantly differ due to the process of carrier thermalization within the localized states. Under conditions of low excitation power and in the limit of high temperatures, the emission spectra $I(E)$ is related to the absorption spectrum by van Roosbroeck-Shockley type of relation(14),

$$I(E) \propto \alpha(E, E_0) \exp(-E/k_B T), \quad T \rightarrow \infty. \quad (4)$$

k_B is the Boltzmann constant and T the lattice temperature. The proportionality constant in the above equation defines a temperature dependent scale factor carrying information about non-radiative pathways. It is evident that the emission spectra in the low and high temperature limits differ essentially by only this exponential factor, that which accounts for carrier thermalization. Furthermore, the behavior between the two limits is expected to be continuous and thus the essence of all car-

rier dynamics is contained in the extent of carrier thermalization. That is, one may just rewrite the exponent as $\exp[-\beta(T)E/k_B T]$ where the parameter $\beta(T) = 0$ and 1 at low and high temperatures respectively. The temperature dependence of the thermalization parameter, $\beta(T)$ contains the essence of all the carrier dynamics through the multiple pathways. Within the constraint of $0 \leq \beta(T) \leq 1$ and $\beta(T_1) \leq \beta(T_2)$, if $T_1 \leq T_2$ the functional form of $\beta(T)$ is not easy to estimate. For simplicity we may approximate it by a sigmoidal function

$$\beta(T) = \frac{1}{1 + \exp[-(T - T_{th})/\Delta]}. \quad (5)$$

T_{th} and Δ are then the only two fit parameters of the model. T_{th} is the temperature when $\beta = 0.5$ and Δ corresponds to the temperature interval over which the transition from a ‘glassy’ to a quasi-equilibrium state occurs. Then, the PL spectrum at a temperature T is

$$I(E, T) \propto \left[\frac{A}{E - E_g} \right]^t e^{-\left[\left(\frac{A}{E - E_g} \right)^{1/k} - \left(\frac{A}{E_0 - E_g} \right)^{1/k} \right]^2 / \sigma^2} e^{-\frac{\beta E}{k_B T}}, \quad (6)$$

with $t = [k + 1 - m + s(1 - \beta)]/k$. $s(1 - \beta)$ is added to insure a correct interpolation between the low and high temperature limits. s denotes exponent of the size dependent capture cross section $\sim a^s$ of dots. $(1 - \beta)$ ensures that the high temperature PL is not explicitly dependent on the trapping efficiency of individual dots. The maximum of this equation, corresponding to the PL peak position at that temperature, is given by the solution of the following equation:

$$\left[\frac{A}{E_p - E_g} \right]^{1/k} - \left[\frac{A}{E_0 - E_g} \right]^{1/k} = \frac{k\sigma^2}{2} \left[\frac{\beta}{k_B T} + \frac{t}{E_p - E_g} \right] \frac{(E_p - E_g)^{\frac{1}{k}+1}}{A^{1/k}} \quad (7)$$

where E_p is the temperature dependent peak energy.

While the values of A , E_g and k were discussed earlier, the value of t is yet to be determined. Within the effective mass picture, the exciton Bohr radius in (bulk) InAs is of the order of 35 nm. This is a bit larger than the typical size of matured InAs/GaAs dots (height 8 nm, pyramid shape, aspect ratio=5). For spherical dots, the oscillator strength $|d_{cv}|^2$ scales inversely with volume(20), i.e. $m=3$, in the limit of small dot sizes. Since our self-assembled dots are neither spherical nor substantially larger or smaller than exciton size, we do not have a clear understanding of the size dependence of the matrix element. We therefore arbitrarily assume a value of m that gives the simplest form to equation 6, i.e. the value for which $k + 1 - m = 0$, with the understanding that the spectral shape of the absorption coefficient, being largely determined by the exponential function, is insensitive to this detail. Similarly, it is not easy to simply estimate the volume dependence of the exciton capture cross section by quantum dots and it is thus simplest to assume that the process of trapping of excitons by quantum dots it is completely random, independent of the quantum dot’s volume. This is the usually made assumption and in the present context leads to a considerable simplification. With these assumptions(21), we have put $t = 0$ in equation 6. Therefore E_0 is the PL peak at zero temperature, corresponding to the mean sized quantum dot in the Gaussian ensemble. On the other hand, the shape

of the absorption spectrum itself is no longer Gaussian and gets skewed toward higher energy, determined by the non-linear relationship between the quantum dot size and transition energy.

There is also the temperature dependent contribution to the shift in the peak of the PL spectrum due to the shrinkage of the gap with temperature, which must be included in any analysis. Fig. 2 (dotted line) shows the temperature dependence of the gap (with the energy zero arbitrarily shifted) for InAs, with Varshni parameters ($a = 0.000276 \text{ eV K}^{-1}$ and $\theta = 93 \text{ K}$ in equation below) taken from literature and therefore the position of the PL peak is given by

$$E(T) = E_p(T) - \frac{aT^2}{\theta + T}. \quad (8)$$

B. Physical basis for the model

Firstly we reiterate that the distribution function for non-resonantly excited carriers within an ensemble of localized states has two distinct regimes of behavior. A low temperatures, the carrier distribution function is proportional to the total density of available states. At very high temperatures, the carriers are in thermal equilibrium with the lattice. In the absence of cooperative ef-

fects, the crossover is expected to be smooth. The temperature dependent function $\beta(T)$, which is defined in Eq.5, describes this crossover.

The introduction of the parameter $\beta(T)$ amounts making the effective carrier temperature different from the lattice temperature while still assuming that the carriers are described by an equilibrium distribution function but with a different effective temperature. The value of the effective carrier temperature is $T/\beta(T)$, always greater than or equal to the lattice temperature. Thus the model is only approximate since it aims at an effective equilibrium description for an essentially non-equilibrium problem. In general, the idea of describing a non-equilibrium distribution by a higher effective temperature is not new. For example, this concept is extensively used in high electric field electron transport studies in semiconductors. In a related study of electron localization in $\text{Ga}_{1-x}\text{In}_x\text{As}_{1-y}\text{N}_y$ quantum wells, we have recently observed that the effective temperature of imperfectly thermalized carriers is indeed higher the lattice temperature(22). The concept of an effective electron temperature for localized carriers in disordered quantum wells was previously proposed in the paper by Gurioli, et al. (14) and further discussed by Runge(12) (section 12a). Runge and coworkers(12) have also used the equilibrium distribution with an effective temperature to describe the results of their simulations of the distribution of partially localized excitons. Furthermore, their simulations also suggest an existence of two distinct regimes, which appear in our model as temperatures above and below T_{th} .

The temperature dependent behavior of the effective temperature T_{eff} may, at first, appear counter-intuitive. The effective temperature is infinite both in the low and high temperature limits. This is because at low temperatures, all the photoexcited carriers are frozen into the states they first get captured into. Thus the carrier distribution function essentially reflects the total density of states. We recall that in the canonical ensemble, temperature is defined in terms of probability of occupation $P(E)$ of a state of energy E through the relation,

$$P(E) = \frac{e^{-E/k_B T}}{Z}. \quad (9)$$

Here Z is the canonical partition function. So it follows that every state has an equal probability of occupation $P(E) = 1/Z$ when the temperature is infinite. This is consistent with the condition we had imposed earlier (in an apparently arbitrary manner) that $\beta = 0$ for carriers to be uniformly distributed over the complete density of states.

It is also tempting to compare our situation with that encountered in the glass transition(23). In context of glasses, the high effective temperature corresponds to an extra configurational entropy contribution. The notion of a crossover temperature is also well-established for glasses and is defined as the temperature at which certain degrees of freedom get frozen. A more microscopic

guess for the function form of the parameter β would require modeling of the barriers associated with the basins of attraction for carriers. Very roughly, the parameters T_{eff} and Δ can be thought to correspond to the glass transition temperature and *fragility* respectively.

Finally, we emphasize that the treatment presented in this paper is restricted to the description of the temperature dependent emission from the ground states of quantum dots.

III. RESULTS AND DISCUSSION

A. Dots with unimodal size distribution

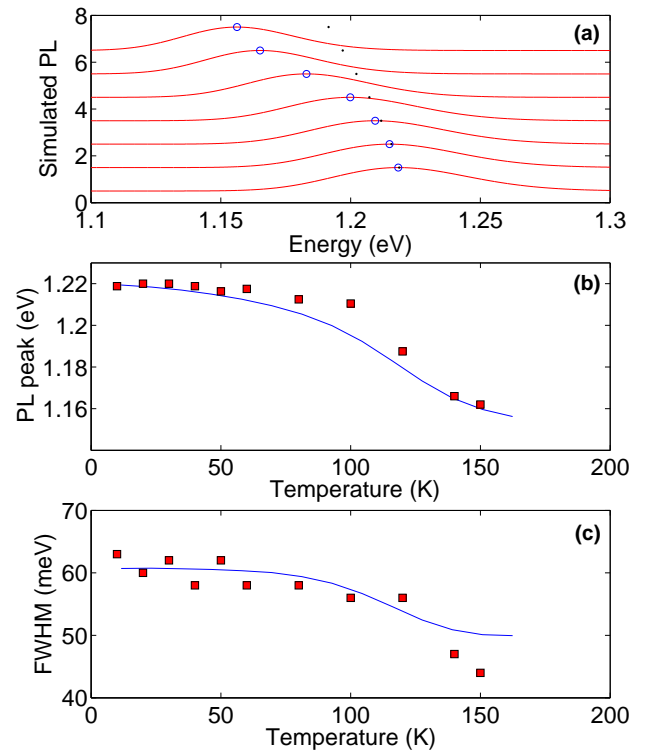


FIG. 1 (a) Simulated photoluminescence spectra at different temperatures, 11K(bottom)-160K (top) in equally spaced temperature intervals. (dots) the expected peak position assuming only the temperature dependent shift in the gap and (circles) the actual peak position. The energy difference between the two corresponds to the Stokes'-like shift (b) Simulated (solid line) and experimental (circles) PL peak energies as a function of temperature. (c) Simulated (solid line) and experimental PL full-widths at half maximum as a function of temperature. The experimental data was taken from reference (8) where the same data is fitted to an alternate model. The theoretical fit depicted here is with the values of $\sigma = 0.8\text{nm}$, $E_0 = 1.22\text{eV}$, $T_{th} = 127\text{K}$, $\Delta = 15\text{K}$.

With the above mentioned assumptions, the normalized PL spectrum is described by the following simple

equation ($t = 0$ and $k = 0.5$ in equation 6)

$$I(E) = I_0(T)e^{-\frac{1}{\sigma^2} \left[\left(\frac{A}{E-E_g} \right)^2 - \left(\frac{A}{E_0-E_g} \right)^2 \right]} e^{-\frac{\beta E}{k_B T}} \quad (10)$$

with $\beta(T)$, defined in equation 5, as the fitting parameter.

To compare with experiments, the energy dependence of PL intensity in equation 10 must be of course also be translated along the energy axis by an amount suggested by equation 8. $I_0(T)$ denotes the temperature dependent scale factor. While this has been previously studied and modelled(24), we do not discuss it further because one usually observes the rather predictable Arrhenius-type activation which may as well be put in by hand. Furthermore, the non-radiative decay channels may depend on a particular sample's past history (e.g., the growth route employed to prepare the sample and the nature of defects) and thus not general enough to be included in a model like this.

Fig.1 shows a comparison of our calculations with the published results of Sanguinetti et al. (figure 4 in reference (8)). The assumption of $\beta \approx 0$ at the lowest temperature fixed $\sigma = 0.8nm$ and $E_0 = 1.219eV$. Then the rest of the fit was accomplished with the values of $\Delta = 15K$ and $T_{th} = 127K$. This fitting procedure is highly constrained since it requires two separate curves to simultaneously fit on the basis of just two free parameters. This should be compared with the rate equation based models, reference (8) for example had eight fitting parameters.

The temperature dependent behaviour of FWHM and peak positions for other values of T_{th} and Δ is depicted in Fig.2. For ease of comparison, the ensemble characteristics, E_0 and σ are the same as those used to generate Fig.1, and only T_{th} and Δ are varied. The model yields a variety of trends at low temperatures. Some of these trends have not only been experimentally observed in the PL from self-assembled quantum dots but seem to be a general characteristic of emission from any inhomogeneous ensemble of localized states. Thus it is tempting to also use the present model to analyse the PL from localized states in the disordered quantum wells as well, in particular the recently much studied dilute nitrides (for a review see e.g., reference (25)) and InGaN (see e.g., (26)) quantum wells.

But to extend this model to localized states in quantum wells would require us to guess an appropriate form of the density of states, which would be a combination of localized band-tail and higher energy extended states. In contrast, for self-assembled quantum dots, all states can be considered to be localized and the density of states can be more or less reliably extracted from the size distribution which in turn is directly accessible to surface probe microscope analysis. Furthermore, the origin of low temperature PL in disordered quantum wells is different from that in quantum dots. While in quantum dots, the PL spectrum at zero temperature can be taken to be proportional to the *total* density of states (all of which are localized and delta-function like), only a small fraction

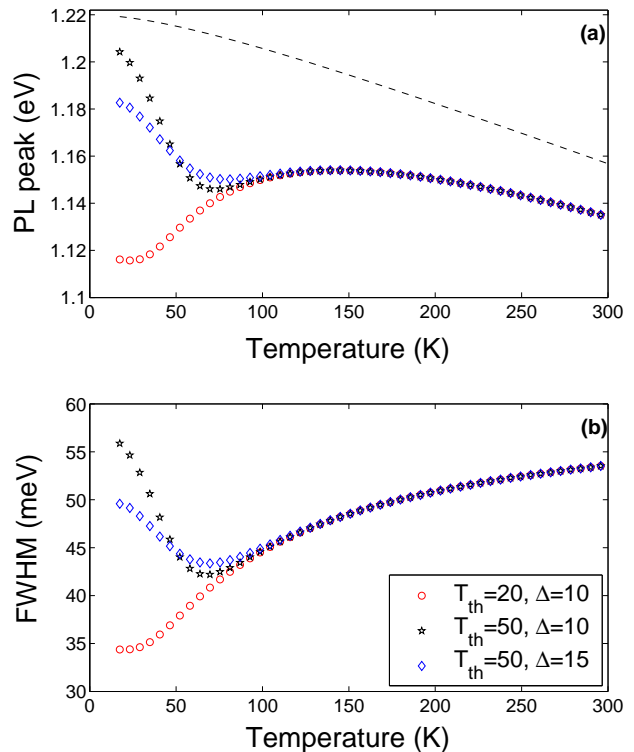


FIG. 2 Calculated temperature dependent characteristics of the PL spectra (a) peak positions (b) FWHM for different values of T_{th} and Δ (in units of Kelvin) with for a fixed values of $\sigma = 0.8nm$ and $E_0 = 1.22eV$. The dotted line in subfigure (a) depicts the temperature dependence of bulk InAs with the energy zero arbitrarily shifted.

(corresponding to the local potential energy minima in a classical sense(27) or the band tail states below the mobility edge) of the total density of states contribute to the low temperature PL in disordered quantum wells.

It is also important to mention that a significant advantage of an effective equilibrium description is that one can continue to use the results from equilibrium theory(28; 29) by just replacing the temperature by effective temperature T_{eff} . The non-monotonic behavior of the linewidths just follows the non-monotonicity of the effective temperature, since the photoluminescence linewidths in equilibrium theory are proportional to $k_B T$. Similarly the temperature dependent “Stokes shift”(28) is described simply by $\sigma^2/k_B T_{eff} \sim (k_B T_{eff})^2/k_B T_{eff} \sim k_B T_{eff}$. This is evident in Fig. 2 where the curves in subfigures (a) and (b) seem to follow each other. Also note that our results are identical to the results in reference (29) in the high temperature limit of $\beta = 1$.

B. Dots with bimodal size distribution

QD ensembles often have a bimodal size distribution, especially during the intermediate stage of growth. This size bimodality also reflects in the low temperature PL

spectra with the appearance of two peaks corresponding to the two QD families. While there have been many experimental studies of the temperature dependence of the two peaks(10; 30; 31; 32; 33; 34), the quantitative theoretical understanding so far has been limited to only the change in the relative intensity of the two peaks as a function of temperature(10; 31). This was done again on the basis of rate equations corresponding to the change in the carrier population in the quantum dots belonging to the two families. Our model is easily extended to

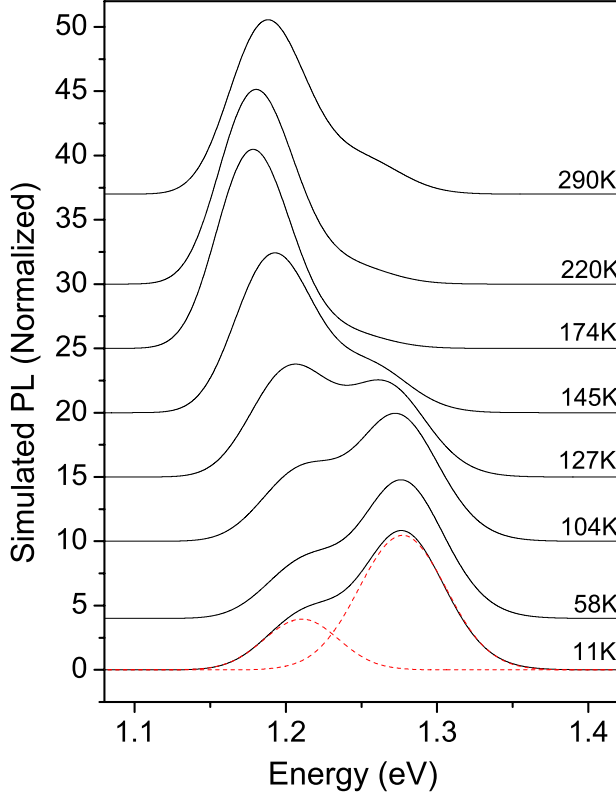


FIG. 3 (Solid line) Simulated photoluminescence spectra at different temperatures for a bimodally size distributed quantum dots ensemble. The curves are normalized such that the total area of each is the same. (Dashed line) 11K spectrum is fitted to two Gaussians. All other curves are also well described as a sum of two Gaussians. Note that the higher energy peak that virtually disappears at 220K is again visible in the 290K spectrum.

describe PL in bimodally size distributed dots, by simply accounting for the modified size distribution which is now a sum of two Gaussian functions, each with a specific mean size and size dispersion around that mean. Denoting by $E_{01,2}$, the energies corresponding to the two mean sizes and the (σ_1 and σ_2) the size dispersions in the two families, we may redefine the optical density of states which we had assumed to be proportional to the absorption coefficient which in turn was proportional to

the PL spectra measured at the lowest temperature as

$$\alpha_{\text{bimod}}(E) = \sum_{i=1,2} \alpha_{0i} e^{-\frac{1}{\sigma_i^2} \left[\left(\frac{A}{E-E_g} \right)^2 - \left(\frac{A}{E_{0i}-E_g} \right)^2 \right]^2}. \quad (11)$$

Here the subscripts 1 and 2 label the two families of dots and the ratio of the constants $\alpha_{01,2}$ is just the relative density of dots in the two families. With this new definition of α_{bimod} , and keeping the rest of the treatment the same, we have plotted simulated PL spectra at different temperatures in Fig.3. The following set of parameter values was used: $\sigma_1 = 0.8\text{nm}$, $\sigma_2 = 0.58\text{nm}$, $E_{01} = 1.22\text{eV}$, $E_{02} = 1.28\text{eV}$, $T_{th} = 150\text{K}$, $\Delta = 15\text{K}$. The ratio of the peak intensities was fixed to $I(E_{01}) : I(E_{02}) = 2 : 1$ at zero temperature. All these values were more or less arbitrarily chosen and supposed to be representative of the ‘typical’ temperature dependent behavior of PL from bimodally size distributed dots.

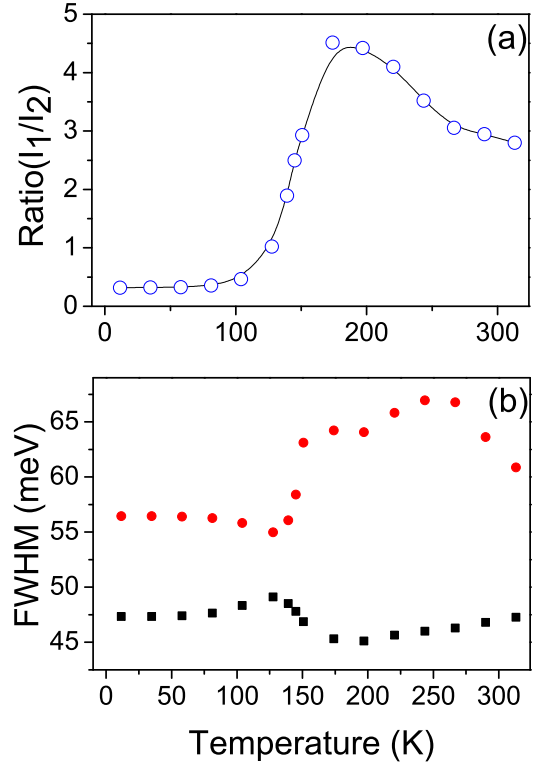


FIG. 4 Analysis of simulated PL spectra, Fig.3. (a) Temperature dependence of the ratio of the integrated intensity of the two peaks. The spectrum shows a carrier transfer to lower energy peak corresponding to larger dots at intermediate temperatures. In accordance with Fig.3, the peak reappears at higher temperatures. Note its qualitative similarity with Fig.4 in the work of Zhang, et al.(10). (b) FWHM of the two peaks at different temperatures.

The spectra in Fig.3 may be compared with the experimentally measured temperature dependent line shapes

from literature, for example Fig.1 from reference (31), Fig.2 in reference (32) and Fig.3 of reference(10).

We note that the experimentally observed trends are reproduced. For ease of analysis, we again ignore the effects of carrier loss to non-radiative decay channels and focus only on the effects of carrier redistribution. Therefore, the curves in Fig.3 are plotted such that the total integrated intensity is same in each case. The spectra in Fig.3 between 11K-150K show the transfer of carriers from smaller to larger dots. The intensity of the higher energy peak is observed to decrease. Since T_{th} is the simulations was 150K, we observe that the thermalization of carriers is nearly complete by 200K. This leads to all the carriers being preferentially in larger dots and a virtual disappearance of the high energy peak. The carrier transfer from the smaller to larger quantum dots was found to be activated. Interestingly, at high enough temperatures, we observe that the high energy peak re-appears when the thermally broadened carrier distribution is so smeared that carriers have sufficient thermal energy to reside on smaller dots. This (somewhat unexpected) behavior has previously been observed in two contexts. Firstly, the plots of the ratio of the intensities between the two peaks (Fig.4 (a)) is qualitatively very similar to the Fig.4 of reference(10). Note that the analysis by Zhang, et al.(10) was based on rate equations and employed many more parameters to simulate a curve similar to Fig.4(a) and had no predictions about the linewidths. Secondly, the reappearance of the high energy feature at high temperature has also been observed in context of pronounced appearance of the wetting layer peak(35) in the high temperature PL spectra from InAs quantum dots.

Finally, the temperature dependence of the positions and the linewidths of the two Gaussians are plotted in Fig.4(b) which shows a small but systematic decrease in the linewidth for the higher energy peak and a corresponding increase in the lower energy peak's linewidth. This feature is generic to the bimodal dots' PL. After 150K, we observe an interesting anomaly as the behavior of the linewidths reverses. This 'anomaly' has also been experimentally observed(32) although not satisfactorily explained.

IV. SUMMARY

We have presented an extremely simple model for the observed anomalies in the temperature dependence of the PL spectra of self-assembled quantum dots. Unlike the previously proposed methods of analysis, we do not invoke a rate equations to model the steady state carrier dynamics but instead introduce a physically motivated factor that parameterizes the degree of thermalization of photoexcited carriers. Since the low and high temperature limits of the carrier distribution are well understood, the process of interpolation allows for an easy visualization of the carrier distribution at different tem-

peratures in terms of this single parameter. Using this model, we could simulate a variety of experimentally observed trends for quantum dots ensembles with both a unimodal and a bimodal distribution.

V. ACKNOWLEDGEMENTS

I thank B.M. Arora for introducing me to self-assembled quantum dots and PL measurements and for many discussions on these topics. I also thank Jayeeta Bhattacharya, Sandip Ghosh and K. L. Narasimhan for very useful comments.

References

- [1] M. Grundmann (Ed.) *Nano-Optoelectronics*, (Springer-Verlag, Berlin 2002).
- [2] M. Sugawara (Ed.) *Semiconductors and Semimetals*, vol 60, Academic Press, San Diego (1999).
- [3] S. Mackowski, G. Prechtel, W. Heiss, F. V. Kyrychenko, G. Karczewski, and J. Kossut, Phys. Rev. B **69**, 205325 (2004).
- [4] Keiichirou Akiba, Naoki Yamamoto, Vincenzo Grillo, Akira Genseki, and Yoshio Watanabe, Phys. Rev. B **70**, 165322 (2004).
- [5] A. Polimeni, A. Patane, M. Henini, L. Eaves, and P. C. Main, Phys. Rev. B **59**, 5064 (1999).
- [6] C. Lobo, N. Perret, D. Morris, J. Zou, D. J. H. Cockayne, M. B. Johnston, M. Gal, and R. Leon, Phys. Rev. B **62**, 2737 (2000).
- [7] Hao Lee, Weidong Yang, and Peter C. Sercel, Phys. Rev. B **55**, 9757 (1997).
- [8] S. Sanguinetti, M. Henini, M. Grassi Alessi, M. Capizzi, P. Frigeri, and S. Franchi, Phys. Rev. B **60**, 8276 (1999).
- [9] Q. Li, S. J. Xu, M. H. Xie, and S. Y. Tong, Europhys. Lett. **71**, 994 (2005).
- [10] Y. C. Zhang, C. J. Huang, F. Q. Liu, B. Xu, J. Wu, Y. H. Chen, D. Ding, W. H. Jiang, X. L. Ye, and Z. G. Wang, J. Appl. Phys. **90**, 1973 (2001).
- [11] A. Patane, A. Levin, A. Polimeni, L. Eaves, P. C. Main, and M. Henini, G. Hill, Phys. Rev. B **62**, 11084 (2000).
- [12] E. Runge, in *Solid State Physics*, edited by H. Ehrenreich and F. Spaepen, (Academic Press, San Diego, 2002), Vol. 57, p. 150.
- [13] For a general introduction to rate equations, see for example, G. Bastard, *Wave Mechanics Applied to Semiconductor Heterostructures*, (Les Editions de Physique, Les Ulis, France, 1992).
- [14] M. Gurioli, A. Vinattieri, J. Martinez-Pastor, and M. Colocci, Phys. Rev. B **50**, 11817 (1994).
- [15] D. Leonard, K. Pond, and P. M. Petroff, Phys. Rev. B **50**, 11687 (1994).
- [16] B. Bansal, M. R. Gokhale, A. Bhattacharya and B. M. Arora, Appl. Phys. Lett. **87**, 203104 (2005).
- [17] M. Grundmann, O. Stier, and D. Bimberg, Phys. Rev. B **52**, 11969 (1995).
- [18] V. Ranjan, V. A. Singh and G. C. John, Phys. Rev. B **58**, 1158 (1998).

- [19] H. Huag and S. W. Koch, *Quantum Theory of the Optical and Electronic Properties of Semiconductor* (World Scientific, Singapore, 1998).
- [20] Y. Kayanuma, Phys. Rev. B **38**, 9797 (1988).
- [21] Although, we have, to keep things simple and in absence of definitive information assumed $t = 0$, the parameter t is in principle measurable through 'Stokes shift' between the peaks of the absorption and the PL spectra.
- [22] B. Bansal, A. Kadir, A. Bhattachraya, B.M. Arora, and R. Bhat, Appl. Phys. Lett. **89**, 032110 (2006); cond-mat/0511282.
- [23] For example, Th. M. Nieuwenhuizen, Phys. Rev. Lett. **80**, 5580 (1998). P. G. Debenedetti and F. H. Stillinger, Nature **410**, 259 (2001).
- [24] E. C. Le Ru, J. Fack, and R. Murray, Phys. Rev. B **67**, 245318 (2003).
- [25] P. J. Klar, Prog. Sol. Stat. Chem., **31**, 301 (2003).
- [26] K. L. Teo, J. S. Colton, P. Y. Yu, E. R. Weber, M. F. Li, W. Liu, K. Uchida, H. Tokunaga, N. Akutsu, and K. Matsumoto Appl. Phys. Lett. **73**, 1697 (1998).
- [27] F. Yang, M. Wilkinson, E. J. Austin, and K. P. O'Donnell, Phys. Rev. Lett. **70**, 323 (1993), ibid. **72**, 1945 (1994) (Erratum).
- [28] P. G. Eliseev, J. Appl. Phys. **93**, 5404 (2003).
- [29] P. G. Eliseev, P. Perlin, J. Lee, M. Osinski, Appl. Phys. Lett., **71**, 569 (1997).
- [30] Y. C. Zhang, C.J. Huang, F.Q. Liu, B. Xu, D. Ding, W.H. Jiang, Y.F. Li, X.L. Ye, J. Wu, Y.H. Chen, and Z.G. Wang, J. Crystal Growth **219**, 199 (2000).
- [31] G. Saint-Girons and I. Sagnes, J. Appl. Phys. **91**, 10115 (2002).
- [32] C.M. Lee, S.H. Choi, J.C. Seo, J.I. Lee, J.Y. Leem, and I.K. Han, J. Korean Phys. Soc. **45** 1615 (2004).
- [33] H.L. Wang, D. Ning, and S.L. Feng, J. Crystal Growth **209**, 630 (2000).
- [34] H. Kissel, U. Muller, C. Walther, W.T. Masselink, Yu I. Mazur, G.G. Tarasov, and M.P. Lisita, Phys. Rev. B, **62**, 7213 (2000).
- [35] A. Patané, A. Polimeni, P. C. Main, M. Henini, and L. Eaves, Appl. Phys. Lett. **75**, 814 (1999).